

# **Automatic Imbalance Reconstruction in Wind Turbines**

**J. Niebsch, R. Ramlau**

**RICAM-Report 2007-37**

# Automatic Imbalance Identification in Wind Turbines

Ronny Ramlau and Jenny Niebsch  
Johann Radon Institute for Comp. and Appl. Math. (RICAM),  
Altenbergerstrasse 69  
4040 Linz, Austria  
Telephone +43 732 2468-5232  
Fax +43 732 2468-5212  
Email: ronny.ramlau@oeaw.ac.at  
jenny.niebsch@oeaw.ac.at

December 18, 2007

## Abstract

Background: Rotor imbalances of a wind power plant can cause severe damages of the plant or its components and thus reduce the lifespan and security significantly. At present balancing of the rotor is a time consuming and expensive process.

Method of approach: We describe a new method for the automatic detection and reconstruction of imbalances in the rotor of a wind turbine. The method is based on a wind turbine model which is derived by the Finite Element Method (FEM). The computation of an imbalance from vibration data measured at the nacelle is an inverse problem.

Results: The proposed reconstruction algorithm works well with artificial and real data and is operating in real time.

Conclusions: The new method reduces the measuring effort for the computation of balancing weights. It can be implemented in a Condition Monitoring System.

## 1 Introduction

In recent years we witnessed the growing importance of renewable energies. Since the 1990th the wind turbine market is fast growing. Wind farm operators expected a lifetime of 20 years for a wind power plant. From the

actual point of view this is not realistic - older plants already show considerable damages on the gearing and other important engine parts. Most of the damages could be avoided if defects and abrasion would be diagnosed in an early state. A major reason for damages lies in the fact that the rotor is imbalanced, i.e. the mass distribution of the rotor is not homogeneous. Imbalances can be caused by manufacturing errors but they can also be developed in the course of time due to profile changes of the blades or water inclusions in the blades' texture. Even small imbalances can cause enormous dynamic loads on the tower as well as on the power train. This leads to nontrivial reparations which need a complex logistic, especially in off-shore areas. Imbalances cause vibrations of the wind turbine with the same frequency as the current rotating frequency. They will usually be detected only if the plant oscillates with large amplitudes, i.e. if the rotating frequency is close to the eigenfrequency of the plant, or if there are already damaged components. In this case an expert team has to balance the machine in a time consuming procedure: In a first step, the vibrations of the turbine, rotating with a frequency as close as possible to the eigenfrequency are measured. Then a test mass has to be placed at one of the blades, and the vibrations are measured again at the same frequency. From this two measurements, the imbalance can be estimated and corresponding balancing weights have to be placed inside the blades. Nevertheless, unusual tower vibrations are only visible if the plant rotates with a frequency close to the first tower eigenfrequency. Otherwise the imbalances may be overlooked for a long time while the dynamic load still affects the engine and the bearings. In a recent project<sup>1</sup> we aimed at the monitoring of the rotor imbalances and an automatic computation of balancing weights from vibration measurements without the necessity of measurements with test masses. The proposed method has mainly two advantages: Firstly, the balancing process can be done in a shorter time, as no time consuming test runs have to be carried out. Secondly, the software based on our algorithm can be integrated in a Condition Monitoring System (CMS). Placing an additional vibrational sensor in the tower, the method will enable us to monitor the imbalance distribution in a long term and allows us to take action whenever it is needed. This is in particular important for offshore power plants as they are not as easily accessible, and maintenance has to be planned in advance. Altogether, the use of a system that monitors the imbalances during operation and indicates when dangerous imbalances are present will save human

---

<sup>1</sup>Elektronische Mechaniküberwachung mittels IT in Windenergieanlagen sponsored by the State of Bremen, Germany

resources and will increase the safety and lifespan of the turbines. The identification of an imbalance from vibration measurements is called an Inverse problem. To solve an Inverse problem we have to be able to handle the Direct problem of computing the vibrations of the plant for a given imbalance first. This can be done using a model of the plant and solving the vibration equation with Finite Element Methods (FEM). Although there already exist several models for wind power plants, we have developed a new and comparable simple one for two reasons: First, in order to find a solution for the Inverse problem the Direct problem has to be solved several times. Thus the computations should be very fast. Second, the imbalance identification algorithm should be applicable for a large variety of plant types. Thus the model should be easily adaptable for each plant type. The fast computation of the Direct problem enables us to solve the Inverse Problem with regularization techniques. In short, the information from the test run with reference imbalances is replaced by the model information, the necessary measurement labor is superseded by mathematical effort.

In Section 2 we will give a mathematical description of imbalances and formulate the Direct problem. Section 3 deals with derivation of the wind turbine model via FEM and its optimization with respect to the first eigenfrequency of the plant. In Section 4 we consider the problem of the reconstruction of the imbalance distribution from vibrational measurements based on the tower model, and discuss a suitable data preprocessing strategy. Section 5 contains results from test computations with the final imbalance reconstruction algorithm. The imbalance identification tool was tested with artificial and real data. The reconstructed imbalances are compared with the reconstruction results from measurements with test mass runs.

## 2 Mathematical problem description

As mentioned in the introduction, a mass imbalance occurs due to an inhomogeneous mass distribution. It can be modelled as

$$p_0 = \Delta m \mathbf{r} \tag{1}$$

with an eccentric mass  $\Delta m$  which is displaced from the barycenter (here the bosses mid point) by the vector

$$\mathbf{r} = r \exp(i\varphi),$$

where  $r$  is the absolute value of  $\mathbf{r}$  and  $\varphi$  is the angle of the imbalance position to a zero mark (usually blade A), see Figure 1. The eccentric mass rotates

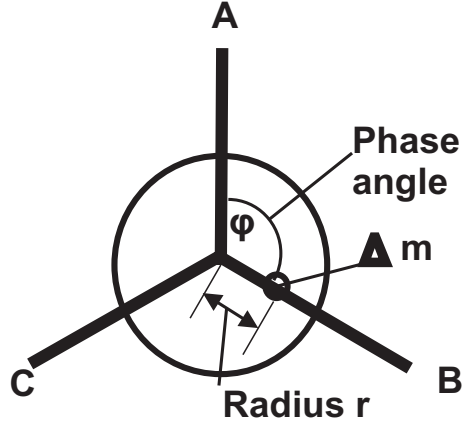


Figure 1: Imbalance model

with a frequency  $\omega$  and causes a harmonic load

$$\begin{aligned} p(t) &= p_0 \omega^2 \exp(i\omega t) \\ &= \omega^2 \Delta m r \exp(i(\omega t + \varphi)). \end{aligned} \quad (2)$$

The load affects the shaft and forces vibrations of the plant. The impact of an arbitrary load (affecting the plant at several points and described by the vector  $\mathbf{p}$ ) on the vibrations  $\mathbf{u}$  depends on the actual plant and can be described by a transfer matrix  $\bar{\mathbf{A}}$ :

$$\mathbf{u} = \bar{\mathbf{A}} \mathbf{p}. \quad (3)$$

$\bar{\mathbf{A}}$  has to be derived from a suitable wind turbine model which will be developed in the next section.  $\bar{\mathbf{A}}\mathbf{p}$  describes the imbalance effect on all nodes of the wind turbine model, i.e.  $\mathbf{u}$  is a vector with as much entries as nodes in the model. However, we can measure the vibrations only at certain nodes  $\mathbf{u}_{sensor}$  where vibration sensors are mounted. Therefore we only need to solve the Direct problem for those entries. Moreover, the imbalance load of the rotor only affects the top node of the plant where the imbalanced rotor is mounted. Hence the imbalance vector  $\mathbf{p}$  has only one nonzero element. This means, we can restrict the matrix  $\bar{\mathbf{A}}$  to a reduced version  $\mathbf{A}$  according to this considerations. Referring to the measured vibrations with  $\mathbf{g} = \mathbf{u}_{sensor}$ , the final equation we have to solve reads

$$\mathbf{g} = \mathbf{A} p \quad (4)$$

with  $p$  from (2).

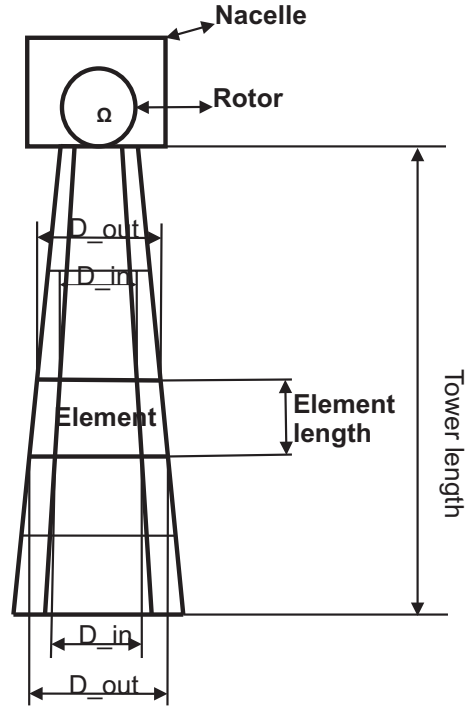


Figure 2: Model of a wind power plant

### 3 Wind turbine model

In this section we want to establish a wind turbine model based on flexible shafts. Usually such a system is described by an equation of the form

$$M\mathbf{u}'' + S\mathbf{u} = \mathbf{p} \quad (5)$$

where  $M$  denotes the mass or inertia matrix,  $S$  the stiffness matrix,  $\mathbf{u}$  the vector of the degrees of freedom,  $\mathbf{p}$  the load vector, The load is directly proportional to  $\omega^2$ , and we have for the frequency the relation  $\omega = 2\pi\Omega$  where  $\Omega$  is the shaft revolution speed.

We only model the tower of the wind turbine as a shaft while the nacelle is treated as point mass as well as the rotor (Figure 2). The imbalance is caused by an eccentric mass rotating with the revolution speed  $\Omega$  (see Figure 1).

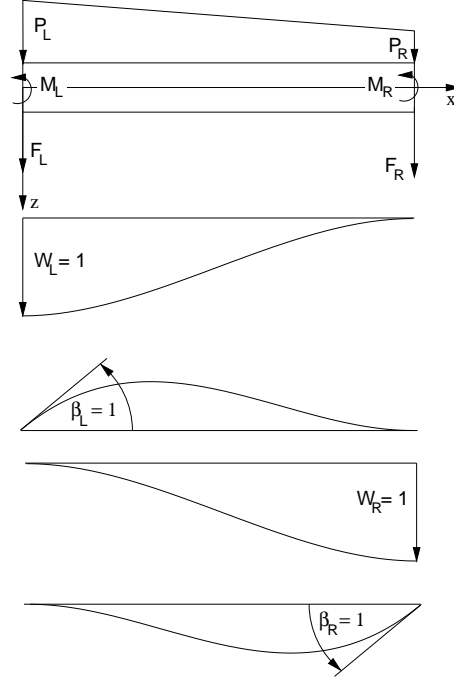


Figure 3: Finite beam elements, loads, shape functions, degrees of freedom

### 3.1 Modelling of a flexible shaft using Finite Elements

The usual technique for calculating the dynamic behavior of flexible shafts is the Finite Element Method (FEM). To get an equation of the type (5), the tower is divided into separate beam elements.

First of all we will discuss a single beam element. All parameters, which refer to a single beam element are marked with a subscript 'e'. For each node the chosen degrees of freedom have to take into account all geometric boundary and transition conditions.

Each finite beam element is treated separately. The motion of the element is described by four shape functions (Figure 3). Their scalable amplitudes are the degrees of freedom  $W_L$ ,  $\beta_L$  of the lower node and  $W_R$ ,  $\beta_R$  of the upper one where  $W$  refers to the transversal displacement and  $\beta$  to the cross section inclination. They are ordered by

$$\mathbf{u}_e^T = [W_L \ \beta_L \ W_R \ \beta_R]. \quad (6)$$

From this ordering results the order of external forces and moments

$$\mathbf{p}_e^T = [F_L \ M_L \ F_R \ M_R]. \quad (7)$$

The characteristics of the beam element are given by its stiffness matrix  $S_e$ , and its inertia or mass matrix  $M_e$ . The influence of a continuous load is described by the element load vector  $\mathbf{p}_e$ . The element matrices and the element load vector are derived by an energy formulation (see [4]). With our choice of shape functions, each of the system matrices  $S_e$  and  $M_e$  are  $4 \times 4$  real matrices. Following [4], the stiffness matrix was derived as

$$S_e = \frac{E \cdot I}{L_e^3} \begin{pmatrix} 12 & -6L_e & -12 & -6L_e \\ -6L_e & 4L_e^2 & 6L_e & 2L_e^2 \\ -12 & 6L_e & 12 & 6L_e \\ -6L_e & 2L_e^2 & -6L_e & 4L_e^2 \end{pmatrix}. \quad (8)$$

The length of the element is represented by  $L_e$ .  $E$  is Young's modulus, for steel we have  $E = 208 \text{ GPa}$ . For circular section beams the transverse moment of inertia  $I$  is given by

$$I = \pi \cdot \frac{D_{e,out}^4 - D_{e,in}^4}{64}$$

with  $D_{e,out}$  for the outer diameter and  $D_{e,in}$  for the inner diameter of the element shaft. The matrix of inertia is given by

$$M_e = \frac{\mu L_e}{420} \begin{pmatrix} 156 & -22L_e & 54 & 13L_e \\ -22L_e & 4L_e^2 & -13L_e & -3L_e^2 \\ 54 & -13L_e & 156 & 22L_e \\ 13L_e & -3L_e^2 & 22L_e & 4L_e^2 \end{pmatrix}. \quad (9)$$

Here  $\mu$  is the translatorial mass per length

$$\mu = \rho \cdot A \quad (10)$$

where  $\rho$  is the density of the material. For steel  $\rho = 7850 \text{ kgm}^{-3}$ .  $A$  is the annulus area. Hence all geometric information needed consists of the length, the outer and the inner diameter of an element.

The element load vector is zero for almost all elements except the last element. The load arising from the imbalance of the rotor is situated at the last (top) node of the model and it affects only the transversal displacement  $W$ . Therefore, the full system load vector has only one entry (see (2)),  $p(t) = \omega^2 \Delta m r \exp(i(\omega t + \varphi))$ , at the last but one position.

To build the full system matrices  $S$  and  $M$ , which combine all beam elements, the element matrices  $S_e$  and  $M_e$  are combined by superimposing the elements affecting the upper node of the  $i$ th element matrix with the ones



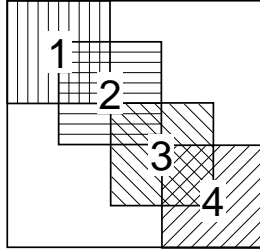


Figure 4: System matrix, superimposed element matrix

belonging to the lower node of the  $(i + 1)$ st element matrix (Figure 4). The sum of rotor mass and nacelle mass have to be added to the last but one diagonal element of the full inertia matrix.

We modelled a wind turbine of the type V80-2MW of the company VESTAS. The nacelle height for this type could be 78 m, 95 m, or 100 m. We were provided with the necessary geometric data of a 100 m construction. For the discretization, the tower was divided into 52 elements. Since the tower bottom is fixed (the degrees of freedom are zero) we got matrices  $M$  and  $S$  of size  $N \times N$  with  $N = 104$ . The nacelle mass is 61.200 kg, the rotor mass is 33.500 kg. The obtained model has a relative simple structure, as e.g. the single blades are not modelled. However, it is sufficient to describe the influence of the imbalance on the tower vibrations, and it has the advantage that it can be evaluated in real time. Moreover, the parameters describing the geometry and the material constants can be changed easily, and thus the model can be generalized to different wind power plants and plant types in a simple way.

### 3.2 Model optimization

For our imbalance reconstruction we depend on measurements of vibrational amplitudes. For a fixed imbalance distribution, the value of the amplitude depends on the operating frequency and assumes its maxima at the eigenfrequencies. Therefore it is very important that the wind power plant model matches the frequency characteristics (amplitude over frequency) or at least the eigenfrequencies of the original plant. Here we can focus on the first eigenfrequency because this is the only one covered by the operating frequency range. We remark that in practise the term eigenfrequency is used for revolution frequency  $\Omega$  instead of the circular frequency  $\omega$ . The eigenfrequency depends on several parameters, e.g. on the damping (which in our case is marginal) or on the underground. But most crucial is the geometry

of the plant tower.

An interval for the first eigenfrequency is given by the manufacturer but its exact value depends on the actual wind power plant. It is usually evaluated from an emergency stop during the final checkup before a plant is plugged into the grid, so it can be assumed to be known.

The model eigenfrequencies can be computed using the assumption  $\mathbf{u}(t) = \mathbf{u}_0 \exp(\omega t)$  and inserting it in the homogenous form of (5). Then we have to solve

$$\omega^2 I \mathbf{u}_0 = -M^{-1} S \mathbf{u}_0, \quad (11)$$

i.e.  $\omega^2$  are the eigenvalues of the matrix  $-M^{-1}S$ . For physical reasons, the eigenvalues are pure imaginary and we get them therefore as

$$\omega_{eig} = \pm \Im(\sqrt{-\text{eig}(M^{-1}S)}).$$

The first rotational eigenfrequency is then given by

$$\Omega_0 = \frac{\min\{\omega_{eig}\}}{2\pi}.$$

The eigenfrequency  $\Omega_0$  depends on the matrices  $M$  and  $S$  which are both quite sensitive to the geometric parameters used as model input. These parameters were the length, inner and outer diameter of each element. Collecting them in the vectors  $\mathbf{L}$ ,  $\mathbf{D}_{in}$ , and  $\mathbf{D}_{out}$ , we have

$$\Omega_0 = \Omega_0(\mathbf{L}, \mathbf{D}_{in}, \mathbf{D}_{out}).$$

Even for parameter disturbances ranging in the manufacturing tolerances we observed large changes of the matrices  $M$  and  $S$ , and hence effects on the eigenfrequency occur. For instance an average change of length and diameter of less than one percent caused a change in the norm of the matrices of about 25%. Thus it seems to be reasonable to change the geometry parameters for a single plant in such a way that the new model eigenfrequency is identical to the measured one. This can be done by a modification of the model parameters due to a minimization of the functional

$$[\mathbf{L}^{opt}, \mathbf{D}_{in}^{opt}, \mathbf{D}_{out}^{opt}] = \arg \min_{\mathbf{L}, \mathbf{D}_{in}, \mathbf{D}_{out}} \|\Omega - \Omega_0(\mathbf{L}, \mathbf{D}_{in}, \mathbf{D}_{out})\|.$$

However, we have to control that the modified parameters still make sense physically. In our case, the first tower eigenfrequency of the V80-2MW model was computed as  $\Omega_0 = 0.28$  Hz which is not contained in the interval given by the manufacturer with  $[0.21 \dots 0.255]$  Hz. For our test computations we have optimized the geometric model parameters to obtain an eigenfrequency of  $\Omega_0 = 0.254$  Hz. As we will see in Section 5, this optimized model produces rather good reconstructions.

## 4 Imbalance identification and data preprocessing

### 4.1 Imbalance identification

From our model we obtain the matrices  $S$  and  $M$  but we still have to derive the operator  $\bar{\mathbf{A}}$  in (3), and  $\mathbf{A}$  in (4). Assuming that a harmonic load  $\mathbf{p} = \omega^2 \mathbf{p}_0 \exp(i\omega t)$  with frequency  $\omega$  causes vibrations of the same frequency, we set

$$\mathbf{u}(t) = \mathbf{u}_0 \exp(i\omega t), \quad (12)$$

where  $\mathbf{u}_0$  is a vector of complex numbers  $u_a \exp(i\varphi)$  containing amplitude and phase of the vibration at every node. Inserting (12) in (5) we can separate the time dependency and get

$$(-\omega^2 M + S) \mathbf{u}_0 = \omega^2 \mathbf{p}_0 \quad \text{or} \quad (13)$$

$$\mathbf{u}_0 = \bar{\mathbf{A}} \mathbf{p}_0 \quad \text{with} \quad (13)$$

$$\bar{\mathbf{A}} = (-M + \omega^{-2} S)^{-1}. \quad (14)$$

$\mathbf{p}_0$  is zero except for the last node with the degrees of freedom  $(W, \beta)$ . The imbalance  $p_0 = \Delta m r \exp(i\varphi)$  arising from an eccentric mass of the rotor only affects the transversal displacement  $W$  which is the last but one degree of freedom. Hence  $\bar{\mathbf{A}}$  can be restricted to the last but one column  $N - 1$  where  $N$  is the number of degrees of freedom in the model.

The vibration sensors can be placed at arbitrary nodes with the numbers  $\mathbf{K} = \{k_1, \dots, k_K\}$ . Therefore,  $\mathbf{A}$  is the restriction of  $\bar{\mathbf{A}}$  to the submatrix with column  $N - 1$  and rows  $\mathbf{K}$ , and has the dimension  $K \times 1$ :

$$\mathbf{g} = \mathbf{A} p_0, \quad (15)$$

$$\text{with } \mathbf{A} = \bar{\mathbf{A}}_{(\mathbf{K}, N-1)}.$$

From measurements we are only provided with noisy data  $\mathbf{g}^\delta$  with a noise level  $\|\mathbf{g} - \mathbf{g}^\delta\| \leq \delta$ . In order to solve (15) approximately for noisy data we have to compute

$$p_0^\delta = \arg \min_p \|\mathbf{A}p - \mathbf{g}^\delta\|^2.$$

This can be done by solving the normal equation. Now the imbalance can be computed as

$$p_0^\delta = (\mathbf{A}^t \mathbf{A})^{-1} \mathbf{A}^t \mathbf{g}^\delta. \quad (16)$$

In our case  $\mathbf{A}^t \mathbf{A}$  is a complex number, and the inverse is simply the reciprocal. However, in more detailed models, e. g. if we also model the power train in the nacelle and allow several parts of the power train to contain imbalances, we have to deal with a matrix  $\mathbf{A}^t \mathbf{A}$  which is usually ill conditioned. Therefore, at this point regularization techniques like in [2] have to be employed.

In practise, there is only one vibration sensor placed in the nacelle, i.e. at the last node of the model. It collects the data for the transversal displacement  $W$  at the last node. This implies that  $\mathbf{A} = \bar{\mathbf{A}}_{(N-1, N-1)}$  is a complex number. The measured values for amplitude and phase can be collected in a complex number  $g_0^\delta$ . Thus the reconstruction problem reduces to a simple division.

$$p_0^\delta = \frac{1}{\mathbf{A}} g_0^\delta.$$

Proceeding in this way the reconstruction error is  $\mathcal{O}(\delta)$ . In particular, the reconstruction can be done in real time. The reconstructed imbalance  $p_0^\delta$  is a complex number where the absolute value corresponds to the product  $\Delta m \cdot r$ , and the phase  $\varphi$  corresponds to the angle of the imbalance position to the rotor blade A (zero mark). To balance the rotor, a balancing weight  $m$  has to be placed at an angle  $2\pi - \varphi$  in a distance  $d$  from the rotor center so that  $m \cdot d$  equals  $\Delta m \cdot r$ . If there is no blade at  $2\pi - \varphi$  the balancing weight has to be split with respect to the vector analysis on the adjoining blades.

## 4.2 Regularization via data preprocessing

The use of our developed model requires vibrational data which are induced by mass imbalances only, i.e. vibrations with the same frequency as the rotating frequency  $\omega_{rot}$ . This would mean that the Fourier expansion of the vibrational data has only one nonzero coefficient for  $\omega = \omega_{rot}$ . However, real vibration signals happen to produce a lot more nonzero Fourier coefficients. They arise by influences not considered in our model as there are e.g. the pass of the blades through the slip stream of the tower, which produces a signal with the frequency  $3 \cdot \omega_{rot}$ . Other causes are gust of wind, aerodynamic imbalances, vibrations of the power train, and the usual data noise with high frequencies. In order to use the measurements, all parts of the signal that do not come from mass imbalances have to be removed. In our approach this is done in a rather simple, but effective way: As the imbalance caused vibrations have a Fourier series expansion with only one nonzero coefficient

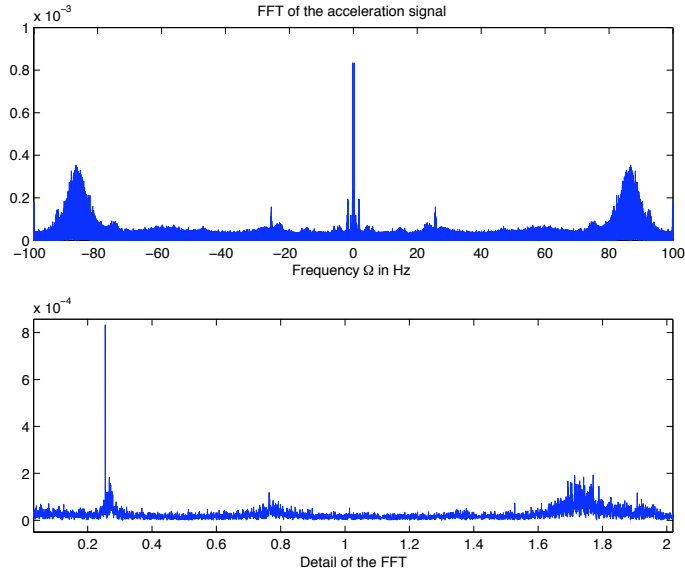


Figure 5: Fourier transform of the measured data (upper image) and a zoom at the rotational frequency  $\omega_{rot} = 0.255Hz$ . Another peak appears at  $3 \cdot \omega_{rot}$  due to the movement of the blades through the slip stream of the tower

at the frequency  $\omega_{rot}$ , we set all other Fourier coefficients in the measured signal to zero and use the filtered signal as input for our inversion process. Figure 5 shows the Fourier coefficients for a vibration signal measured with an acceleration sensor during the operation of the plant with a frequency  $\omega_{rot} = 0.255Hz$ . The detailed view displays the coefficients near the rotating frequency. Apart from the maximal coefficient at  $\omega_{rot}$  we can observe a local maximum at  $3 \cdot \omega_{rot}$  as explained above.

The described preprocessing of the data can be interpreted as a projection of the data to the modelled problem. Moreover, it can be also understood as a denoising process, as the high frequency part of the signal is removed before the inversion. Thus, the whole inversion process can be understood as a regularization in the sense of [1] and [5].

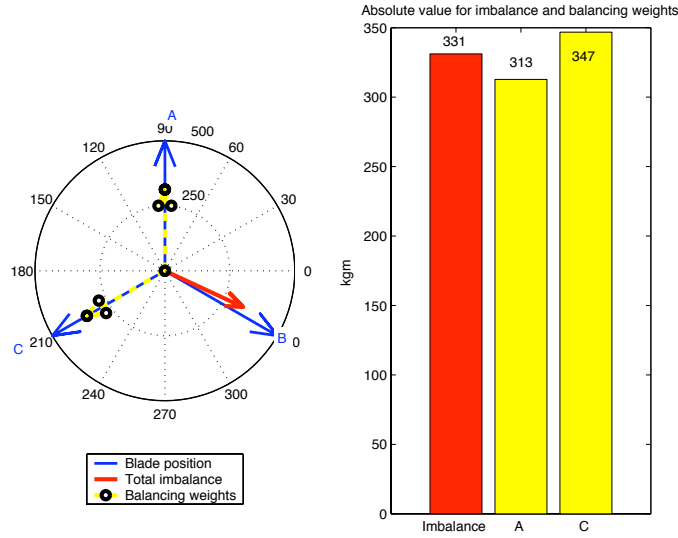


Figure 6: Reconstruction and balancing weights for an imbalance of 350 kgm at blade B with a data noise level of 10 %

## 5 Test computations

### 5.1 Reconstruction with artificial data

As a first test of the algorithm we have assumed an imbalance of 350 kgm at the blade B of a V80-2MW. This is a realistic value. The vibrational data for such an imbalance were produced by forward computation with  $\mathbf{A}$  and disturbed with a data error level of 10%. The vibration amplitude is about 0.1 m (see Figure 7, dashed line) because with  $\Omega = 0.25$  Hz we have chosen a revolution frequency close to the eigenfrequency of the tower. Again this is a realistic value as engineers confirm. The reconstruction and the related balancing weights are shown in Figure 6. Placing the balancing weights (e.g. 313 kg at a distance of 1 m in blade A, and 173,5 kg at distance of 2 m at blade C), the vibration amplitude will be reduced significantly as shown in Figure 7 (solid line).

The reconstruction error  $\frac{\|p_0^\delta - p_0\|}{\|p_0\|}$  is about 10% as expected for a data noise level of the same amount.

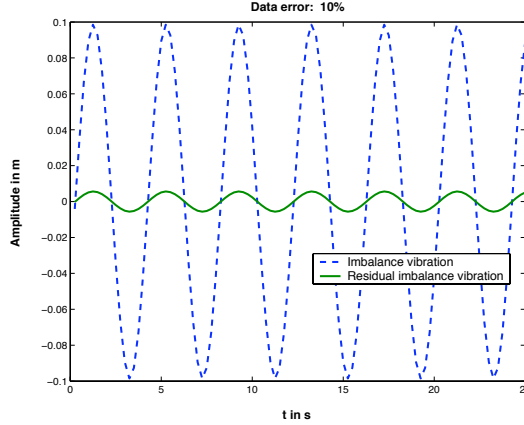


Figure 7: Vibrational data for an imbalance of 350 kgm at blade B and vibrations after balancing with the computed balancing weights

## 5.2 Reconstruction with real data

After several successful test computations with artificial data we tested the algorithm with real data. They were provided by the Company Deutsche WindGuard Dynamics Berlin which is a leading provider of imbalance services based on measurements with test weight runs. There were only data available for a 95m construction of a V80-2MW with a first eigenfrequency of 0.269 Hz. Thus we changed the model geometry and optimized the model to fit the eigenfrequency.

The raw vibrational data which were collected with an acceleration sensor at a rotational frequency  $\Omega_{rot} = 0.255$  Hz are shown in Figure 8.

Data of a trigger signal (one impulse per revolution) were also provided. Amplitude  $A$  and phase  $\varphi$  of the acceleration vibration at  $\Omega_{rot}$  were computed as described in the former section. To obtain the related distance amplitude  $g_a$  and phase  $\varphi_g$  for  $g(t) = g_a \cos(2\pi\omega t + \varphi_g)$  we have used the following relations which arise from a double integration of the acceleration signal:

$$g_a = \frac{A}{(2\pi\omega)^2}, \quad (17)$$

$$\varphi_g = \varphi + \pi. \quad (18)$$

The filtered distance vibration  $g(t) = g_a \cos(2\pi\Omega t + \varphi_g)$  is plotted in Figure 9. The reconstruction with the preprocessed data resulted in a reconstructed imbalance of 94 kgm. The imbalance computed by Dynamics using test

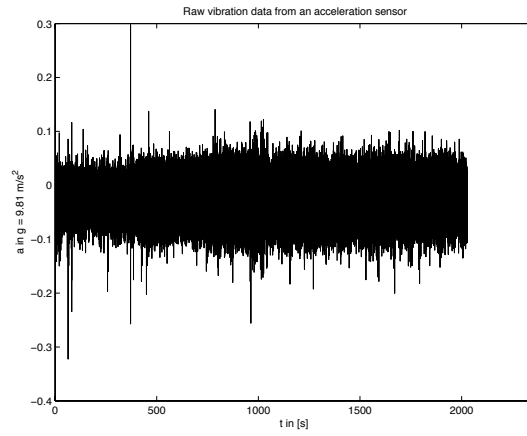


Figure 8: Raw acceleration data for a Vestas V80-2MW wind power plant, provided by the company Deutsche WindGuard Dynamics

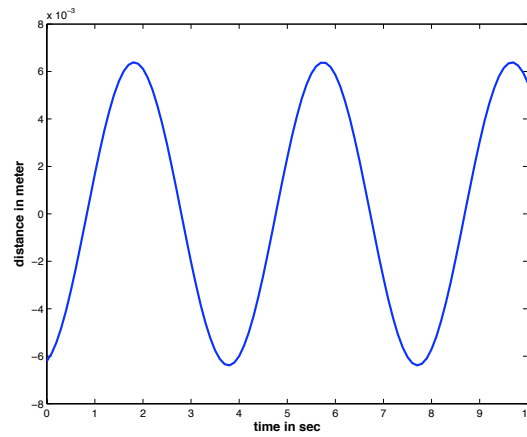


Figure 9: Preprocessed distance data, obtained from the raw data shown in Figure 8



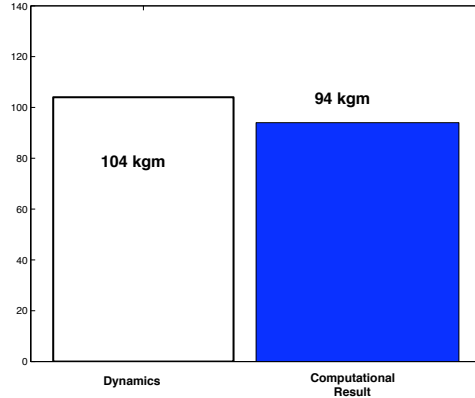


Figure 10: Imbalance values for different methods

runs and test weights was given with 104 kgm, see Figure 10. A confidence interval of 20-30 % for their results was given. Thus our result is contained in that interval. Because Dynamics works with relative data samples there was no zero mark given. Therefore we have reconstructed the imbalance position in relation to the trigger position with  $193^\circ$ . The total amount of computational time was in the range of seconds.

## 6 Conclusion

The safely and economic operation of a wind turbine requires a well balanced rotor. Therefore the detection of imbalances and their removal is an important task for the monitoring of a wind power plant. Presently the balancing process requires an extensive and time consuming measurement procedure.

Our new imbalance reconstruction method, which is based on a mathematical model of the wind power plant reduces the effort for balancing significantly. The method was successfully tested with artificial and real data. The used model can be easily generalized to different types of wind power plants, and can therefore be integrated into Condition Monitoring Systems. The method requires vibrational data from measurements with constant rotor frequency. However, usually the frequency is variable and changes according to the wind conditions. A way to overcome this difficulty is by running the system at constant frequency (which can be done using the control system of the plant) or by taking long measurement series and

extracting intervals where the plant runs with almost constant frequency. Nevertheless, the reconstruction of imbalances for time variable frequencies should be an interesting topic for future investigations.

## References

- [1] Cohen, A., Hoffmann, M. and Reiss, M., "Adaptive wavelet Galerkin methods for linear inverse problems", SIAM J. Numerical Analysis, **42**(4), 2004.
- [2] Dicken, V., Maass, P., Menz, I., Niebsch, J. and Ramlau, R., "Nonlinear inverse unbalance reconstruction in rotor dynamics", Inverse Problems in Science & Engineering, **13**(5), pp. 507-543, 2005.
- [3] Engl, H. W., Hanke, M. and Neubauer, A., Regularization of Inverse Problems. Kluwer, Dordrecht, 1996.
- [4] Gasch, R. and Knothe, K., Strukturdynamik 2. Springer, Berlin, 1989.
- [5] Klann, E., Maass, P. and Ramlau, R., "Two-Step regularization methods for linear inverse problems", Journal of Inverse Ill-Posed Problems, **14**(5), pp. 583–607, 2006.
- [6] Louis, A. K., Inverse und schlecht gestellte Probleme. Teubner, Stuttgart, 1989.
- [7] Ramlau, R., "Morozov's Discrepancy Principle for Tikhonov regularization of nonlinear operators", Numer. Funct. Anal. and Optimization, **23**(1&2), pp. 147–172, 2002.
- [8] Ramlau, R., "A steepest descent algorithm for the global minimization of the Tikhonov– functional", Inverse Problems **18**(2), pp. 381-405, 2002.
- [9] Ramlau, R., "TIGRA—an iterative algorithm for regularizing nonlinear ill-posed problem", Inverse Problems **19**(2), pp. 433-467, 2003.
- [10] Scherzer, O., "The use of Morozov's discrepancy principle for Tikhonov regularization for solving nonlinear ill-posed problems", Computing, **51**, pp. 45-60, 1993.